Entropy in central Au + Au reactions between 100 and 400A MeV

M. Dželalija,[10] N. Cindro,[13] Z. Basrak,[13] R. Čaplar,[13] S. Hölbling,[13] M. Bini,[5] P. R. Maurenzig,[5] A. Olmi,[5] G. Pasquali,[5] G. Poggi,[5] N. Taccetti,[5] C. Cerruti,[11] J. P. Coffin,[11] R. Donà,[11] P. Fintz,[11] G. Guillaume,[11] A. Houari,[11] F. Jundt,[11] C. Kuhn,[11] F. Rami,[11] R. Tezkratt,[11] P. Wagner,[11] J. Biegansky,[9] R. Kotte,[9] J. Mösner,[9] W. Neubert,[9] D. Wohlfarth,[9] J. P. Alard,[3] V. Amouroux,[3] N. Bastid,[3] L. Berger,[3] I. M. Belayev,[7] S. Boussange,[3] A. Buta,[1] P. Dupieux,[3] J. Erö,[2] Z. Fodor,[2] L. Fraysse,[3] A. Gobbi,[4] N. Herrmann,[6] K. D. Hildenbrand,[4] M. Ibnouzahir,[3] J. Kecskemeti,[2] P. Koncz,[2] Y. Korchagin,[7] M. Krämer,[4] A. Lebedev,[7] I. Legrand,[1] V. Manko,[8] G. Mgebrishvili,[8] D. Moisa,[1] G. Montarou,[3] I. Montbel,[3] D. Pelte,[6] M. Petrovici,[1] P. Pras,[3] V. Ramillien,[3] W. Reisdorf,[4] D. Schüll,[4] Z. Seres,[2] B. Sikora,[12] V. Simion,[1] S. Smolyankin,[8] U. Sodan,[4] M. Trzaska,[6] M. A. Vasiliev,[8] J. P. Wessels,[4] T. Wienold,[6] Z. Wilhelmi,[12] and A. V. Zhilin[7]

[1] *Institute for Physics and Nuclear Engineering, Bucharest, Romania*
[2] *Central Research Institute for Physics, Budapest, Hungary*
[3] *Laboratoire de Physique Corpusculaire, Clermont-Ferrand, France*
[4] *Gesellschaft für Schwerionenforschung, Darmstadt, Germany*
[5] *I.N.F.N. and University of Florence, Florence, Italy*
[6] *Physikalisches Institut der Universität Heidelberg, Heidelberg, Germany*
[7] *Institute for Experimental and Theoretical Physics, Moscow, Russia*
[8] *Kurchatov Institute for Atomic Energy, Moscow, Russia*
[9] *Forschungzentrum, Rossendorf, Germany*
[10] *Department of Physics, University of Split, Split, Croatia*
[11] *Centre de Recherches Nucléaires, IN2P3-CNRS, Université Louis Pasteur, Strasbourg, France*
[12] *Institute of Experimental Physics, Warsaw University, Warsaw, Poland*
[13] *Rudjer Bošković Institute, Zagreb, Croatia*

(Received 20 January 1995)

The ratio of the total charge bound in fragments with Z between 2 and 15 to the hydrogen yield, $(\sum_2^{15} M_i Z_i)/M_H$, has been measured, and the neutron-to-proton ratio n/p has been estimated from the data of central Au + Au reactions between 100 and 400A MeV, measured with the phase I setup of the detector system FOPI at the GSI, Darmstadt, in the polar-angle range between 7° and 30°. These two quantities were used to determine the entropy per nucleon S/A by comparing them with the predictions of the FREESCO code. The analysis allows the simultaneous extraction of the values of the baryonic entropy, temperature, and collective flow. The extracted values are in good agreement with the values obtained in earlier FOPI studies and, for the baryonic entropy, with recent hydrodynamic calculations.

PACS number(s): 25.75.+r, 25.70.Pq

I. INTRODUCTION

The equilibration of hot, dense nuclear matter created in high-energy heavy-ion collisions plays an important role in the description of the processes. It is, hence, interesting to understand whether, with time, the colliding system eventually reaches some kind of local or even global thermal equilibrium. If it does, it would be of importance to find a variable that describes the properties of the system in equilibrium.

A thermodynamic analysis of the system in terms of temperature and density is not simple, because these quantities change quickly with time. It is generally assumed that the quantity that remains almost unchanged through the final stages of the interaction is entropy [1]. Entropy grows rapidly during the first stage of the collision, but once the equilibrium is reached the rate of entropy production becomes small. Thus a measurement of this physical quantity yields information about the state of hot and dense matter after at least local equilibrium is established. The first study of the entropy in heavy-ion collisions was performed by Siemens and Kapusta, who calculated it from the deuteron-to-proton ratio for the Ne + NaF and Ar + KCl systems at 400A and 800A MeV [2].

For a system with a probability p_i to be found in a microstate i, the entropy is defined as

$$S = -k \sum_i p_i \ln p_i, \tag{1}$$

where k is the Boltzmann constant. For a nonequilibrated system of independent fermions, this expression leads to

$$S = -k \int \frac{d\vec{p}d\vec{r}}{h^3}[f \ln f + (1-f)\ln(1-f)], \quad (2)$$

where h is the Planck constant and f is the single-particle distribution function. This expression is applicable when the temperature of the system is much higher than the binding energy per particle. Using expression (2) and the approximations given in Ref. [3], it is possible to derive the well-known Siemens-Kapusta [2] entropy formula

$$S/A = 3.945 - \ln R_{dp}, \quad (3)$$

where R_{dp} is the deuteron-to-proton yield ratio. Since the independent particle model is not a good description of low-energy collisions, it is clear that the above formula works better for intermediate and high collision energies. Moreover, as the experimental d/p ratio is seriously contaminated by decays from nuclear resonances, this formula should be taken with some reserve at all energies.

In several subsequent experimental papers [4–10], the value of entropy was determined for various nuclear systems and projectile energies using the quantum statistical model (QSM) [11] and different global observables. The determination of entropy from exclusive measurements of intermediate mass fragments (IMF's) up to $Z = 15$ ($3 \leq Z \leq 15$) was first performed by Kuhn *et al.* [12] using the Au + Au FOPI Collaboration data. In their study [12], various observables characterizing the dM/dZ fragment multiplicity distributions were compared with those calculated using the QSM. The entropy values obtained in [12] were lower than those reported in earlier publications; the origin of this difference is well understood and will be discussed later. The results of Ref. [12] were, however, in good agreement with low-viscosity hydrodynamic calculations [13].

Since the determination of entropy is obviously model dependent, it is interesting to start from a given set of experimental data and compare the entropy values extracted by means of different models describing the breakup of an excited source. Thus we decided to use the data from the same set of Au + Au experiments as in [12] and, instead of using the QSM, analyze the data in terms of the fragmentation by explosion/evaporation simulation code (FREESCO) [14]. It has been shown [15] that the predictions of these two models coincide at intermediate and high beam energies, in spite of the fact that classical statistics is used in the FREESCO. Figure 1, in fact, shows that the charge distributions dM/dZ obtained from the QSM are close to that obtained from the FREESCO without filter, for the same values of the density. This code, however, works as an event generator and thus has the advantage that its output distributions can be sent through a filter matched to the acceptance of the particular detection configuration. In addition, the Coulomb interaction is explicitly treated in the FREESCO.

For the extraction of S/A, two physical quantities were used: (i) the total charge bound in fragments with Z between 2 and 15 to hydrogen, $(\sum_2^{15} M_i Z_i)/M_H$, where M_i and M_H denote the multiplicities of the respective elements in the event, measured at laboratory polar angles between 7° and 30°, and (ii) the neutron-to-proton yield ratio n/p evaluated using an expression that will be introduced later. Thus in this paper we extend the analysis performed in [12] to a different simulation code and extract the S/A values using two new variables. To allow a comparison with Ref. [12], we used two rapidity conditions: (a) for $(y \geq 0)_{\text{c.m.}}$ (the forward hemisphere) and (b) for $(0 \leq y \leq 0.6y_p)_{\text{c.m.}}$ (the midrapidity region).

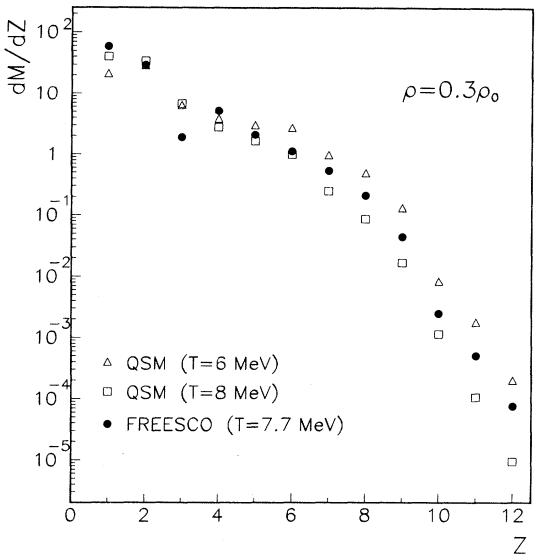

FIG. 1. Charge distributions obtained from the FREESCO without filter (full circles), compared with the distributions from the QSM for two temperatures, $T = 6$ MeV (triangles) and $T = 8$ MeV (squares).

The paper is organized as follows. Section II briefly describes the results of the measurement of central Au + Au collisions. The values of the baryonic entropy S/A extracted from the comparison of the two ratios with those calculated using the modified FREESCO code are presented in Sec. III and discussed in Sec. IV. A summary is given in Sec. V.

II. EXPERIMENTAL RESULTS

The experiments to study central Au + Au collisions in the energy range from $100A$ to $400A$ MeV were performed at the GSI, Darmstadt, using the phase I setup of the 4π-detector system FOPI. This system was described elsewhere [16–18]. It consists of three main components: the plastic wall, the cluster detector shell, and eight ΔE-E particle telescopes. The plastic wall and the cluster detector shell cover the polar-angle range between 1° and 30°, with full azimuthal span, allowing element identification of particles with $Z \leq 15$, with detection thresholds from $15A$ MeV for $Z = 1A$ to $50A$ MeV for $Z = 15$. The telescopes could be moved in a horizontal plane between 6° and 90°. They identified, with even lower thresholds, the charge of reaction products up to $Z \approx 20$ and, for lighter products, also their mass. For the present analysis, however, we used the Z distributions obtained only

from the so-called outer plastic wall and its ionization-chamber cluster detector, which covered the polar-angle range from 7° to 30°. The d/p and t/p ratios, used in Eq. (6), were measured by the telescopes.

To select central events, three different selection criteria have been used so far: (i) the charged-particle multiplicity, measured in the polar-angle range between 7° and 30°, starting at half of the value of the distribution plateau [19] (the PM5 criterion); (ii) the transverse momentum directivity

$$D = \left[\frac{\left|\sum_i \vec{p}_\perp^{(i)}\right|}{\sum_i \left|\vec{p}_\perp^{(i)}\right|}\right]_{(y\geq 0)_{\text{c.m.}}}, \tag{4}$$

taken with the limit $D \leq 0.2$ and combined with PM5 [20,21] (the PM5D1 criterion); and (iii) the transverse-to-longitudinal kinetic energy ratio (ERAT) in the center of mass [22], given by

$$\left[\frac{\sum_i E_\perp^{(i)}}{\sum_i E_\parallel^{(i)}}\right]_{(y\geq 0)_{\text{c.m.}}}, \tag{5}$$

gauged to as many events as for PM5 for a given set of collected events (the ERAT5 criterion).

Figure 2 shows the $(\sum_2^{15} M_i Z_i)/M_H$ ratio as a function of incident energy for, respectively, the ERAT5, PM5, and PM5D1 selection criteria, each with two rapidity conditions, $(y \geq 0)_{\text{c.m.}}$ and $(0 \leq y \leq 0.6y_p)_{\text{c.m.}}$. The values of the rapidities in these conditions were chosen to allow a comparison with the results of Ref. [12].

The neutron-to-proton yield ratio was not measured directly. It was calculated from the available data using the expression

$$n/p \approx \frac{197}{79}\left(1+\frac{d}{p}+\frac{t}{p}\right)\left(1+\frac{\sum_2^{15} M_i Z_i}{M_H}\right) - \left(1+2\frac{d}{p}+3\frac{t}{p}\right) - 2\left(1+\frac{d}{p}+\frac{t}{p}\right) \times \left(\frac{\sum_2^{15} M_i Z_i}{M_H}\right), \tag{6}$$

where p, d, and t are, respectively, the proton, deuteron, and triton multiplicities determined using the telescope data extrapolated to the same solid angle covered by the charged-particle detectors (entire azimuth and polar angles between 7° and 30°). To obtain Eq. (6), we assumed $A = 2Z$ for all emitted charged fragments with $2 \leq Z \leq 15$. This assumption was made in view of the average trend of nuclei with $Z = 2$ to 15. The derivation of Eq. (6) is given in the Appendix. The neutron-to-proton yield ratios obtained from the data using Eq. (6) are shown in Fig. 3, with the same symbols as in Fig. 2. The error bars in these figures are estimated due to the high-energy thresholds of the outer plastic wall and its ionization-chamber cluster detector. The bars present a maximum of allowed uncertainty.

A cross-check of the above method to evaluate the n/p yield ratio was to simultaneously calculate the ratio from, respectively, neutron and proton emission rates given by the FREESCO and from Eq. (6), but using the values of the ratios appearing in this expression as given by the FREESCO. The sets of values [for $(y \geq 0)_{\text{c.m.}}$ only] are shown in the inset of Fig. 3 [asterisks: ratios calculated from the FREESCO yields; diamonds: those calculated using Eq. (6)]. The agreement is satisfactory, showing the applicability of the method.

Figures 2 and 3 show that both quantities, the ratio of the total charge bound in fragments with Z between 2 and 15 to hydrogen production, $(\sum_2^{15} M_i Z_i)/M_H$, and the evaluated neutron-to-proton ratio n/p, when extracted from the midrapidity region $(0 \leq y \leq 0.6y_p)_{\text{c.m.}}$, are systematically larger than the same quantities extracted from the whole half-space of rapidity $(y \geq 0)_{\text{c.m.}}$.

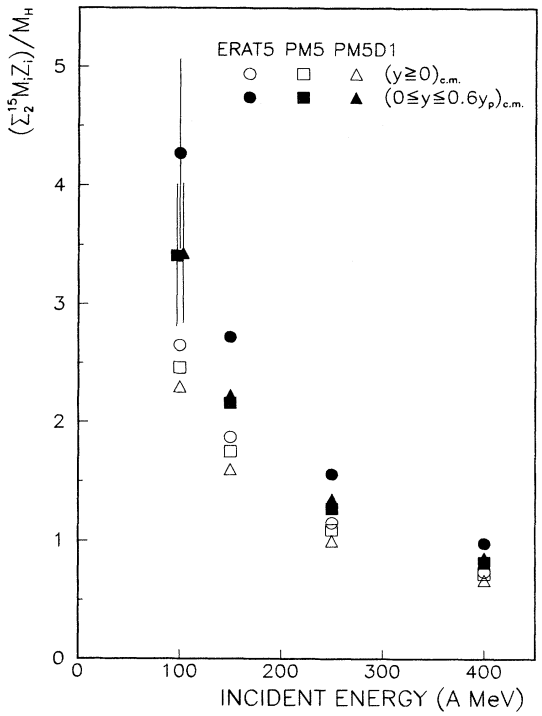

FIG. 2. Ratio of the total charge bound in fragments with Z between 2 and 15 to hydrogen production, $(\sum_2^{15} M_i Z_i)/M_H$, as a function of beam energy, shown for the ERAT5 (circles), PM5 (squares), and PM5D1 (triangles) selection criteria. The open symbols correspond to the full rapidity hemisphere $(y \geq 0)_{\text{c.m.}}$ and the full ones to the midrapidity region $(0 \leq y \leq 0.6y_p)_{\text{c.m.}}$. The experimental uncertainties are mainly due to the high-energy thresholds of the outer plastic wall and its ionization-chamber cluster detector.

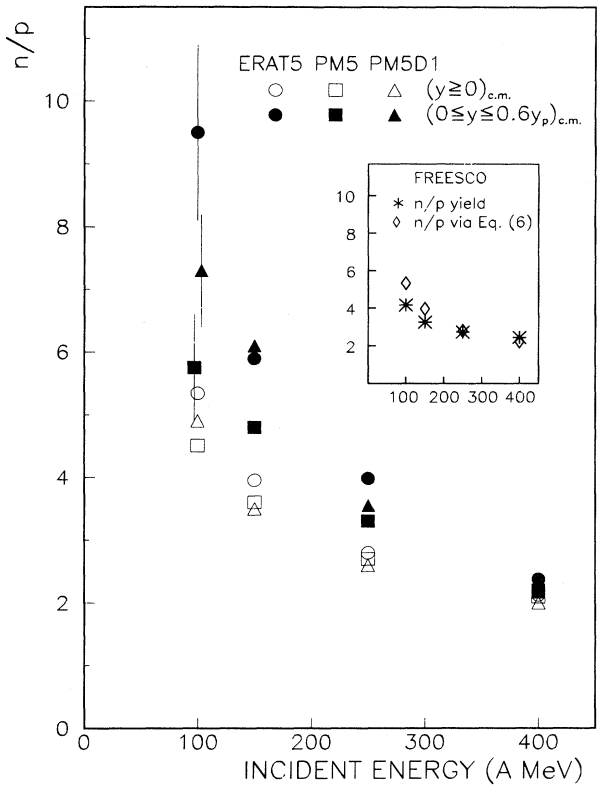

FIG. 3. Same as Fig. 2 for the neutron-to-proton yield ratio n/p evaluated from the data using Eq. (6). For the inset see text.

(relative decrease in the number of light particles emitted in the midrapidity region).

Since PM5D1 needs a double cut, it considerably reduces the statistics of the telescope yields, which were necessary to determine the n/p ratio in Eq. (6). On the other hand, since ERAT5 is as selective as PM5D1 and not so prejudicial to the number of events, in the analysis that follows we use only the ERAT5 criterion to select central events.

III. ENTROPY DETERMINATION FROM COMPARISON WITH THE MODIFIED FREESCO

Depending on the impact parameter, the FREESCO code [14] describes a symmetric collision system as a single or as a triple source (the projectile and target "spectators" and the "participant"). Each source is characterized by its number of nucleons, its charge, and its four-momentum. The disassembly of the sources is described as a two-stage process. If the excitation energy of a source is above the disassembly threshold, the source can explode rapidly into pions, nucleons, and fragments. Sources with excitation energy below the disassembly threshold and metastable products of the explosion are assumed to deexcite on a slower time scale via sequential light-particle emission. The γ decay, which is expected to modify the fragment momentum only slightly, is neglected. In the standard version of FREESCO [14, 23], only the production of fragments with $A \leq 16$ was considered. However, faced with the experimental evidence for the production of a large variety of clusters even in the most central collisions, Fan *et al.* [24] extended the FREESCO to include all fragments with $Z \leq 15$ appearing in the *Table of Isotopes* [25]. Subsequently, collective motion was also introduced, assuming that the total energy of a fragment consisted of a random, undirected thermal energy and a collective-flow energy (E_x^F, E_y^F, E_z^F) [26].

In the present paper we use the single-source mode of the modified FREESCO code. All calculations were performed for various values of the temperature T, obtained by varying the collective-flow energy (E_x^F, E_y^F, E_z^F) until FREESCO reproduces the $(\sum_2^{15} M_i Z_i)/M_H$ and n/p ratios calculated from the data by using Eq. (6). For simplicity, we assumed an isotropic flow distribution $E_x^F = E_y^F = E_z^F = E^F/3$. The freeze-out density of $\rho = 0.3\rho_0$ (corresponding to $\chi = 2.82$) is used following Refs. [12] and [27]. The Coulomb interaction was included. Since the FREESCO was designed to simulate nuclear collisions in a Monte Carlo framework, the calcu-

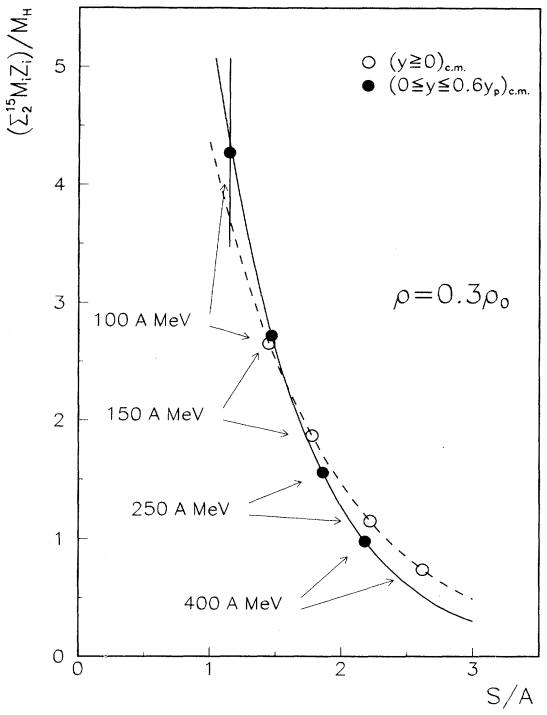

FIG. 4. Ratio of the total charge bound in fragments with Z between 2 and 15 to hydrogen production, $(\sum_2^{15} M_i Z_i)/M_H$, calculated from the modified FREESCO with $\rho = 0.3\rho_0$, as a function of baryonic entropy for $(y \geq 0)_{\text{c.m.}}$ (dashed curve) and for the midrapidity region $(0 \leq y \leq 0.6y_p)_{\text{c.m.}}$ (solid curve). The ratios extracted from the data for different beam energies and rapidity conditions are shown as open circles for $(y \geq 0)_{\text{c.m.}}$ and full circles for $(0 \leq y \leq 0.6y_p)_{\text{c.m.}}$ (ERAT5 conditions apply).

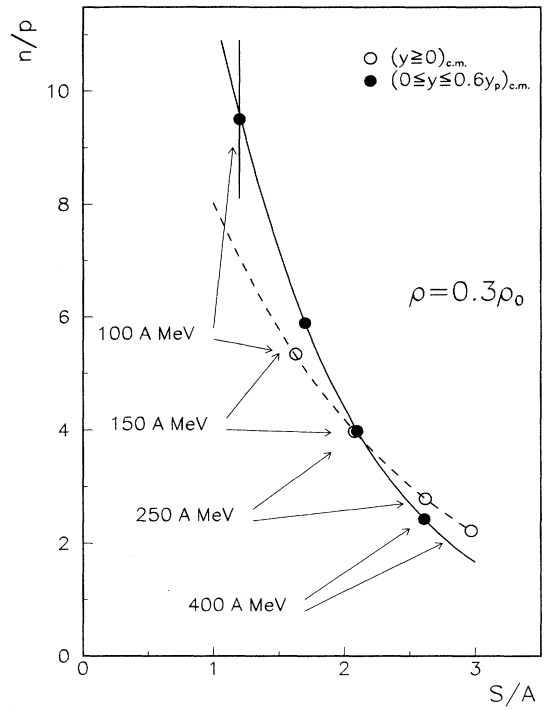

FIG. 5. Same as Fig. 4 for the neutron-to-proton yield ratio n/p evaluated from the data using Eq. (6).

lations were first filtered [28] to match the acceptance of the particular FOPI detection configuration used. The dashed curves in Figs. 4 and 5 are obtained from the FREESCO calculation selecting particles with the rapidity condition $(y \geq 0)_{\text{c.m.}}$, and the solid curves are obtained with $(0 \leq y \leq 0.6y_p)_{\text{c.m.}}$.

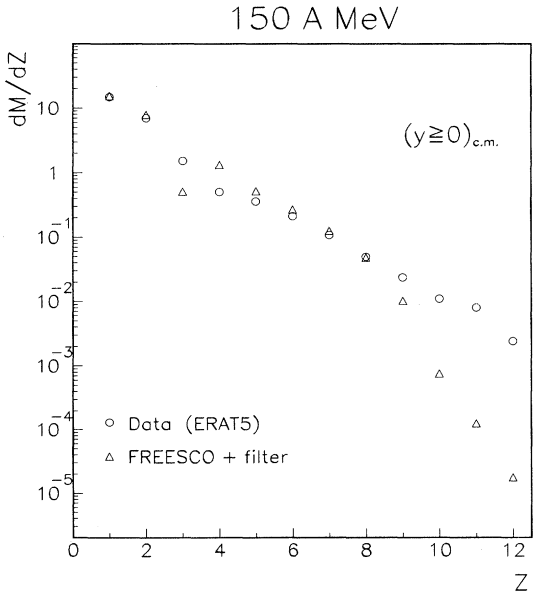

FIG. 6. Charge distributions dM/dZ for central Au + Au reactions at 150A MeV, measured (circles) and calculated with the FREESCO (triangles). In the calculations, the freeze-out density was taken as $\rho = 0.3\rho_0$ and the temperature $T = 7.7$ MeV.

The values of the $(\sum_2^{15} M_i Z_i)/M_H$ and n/p ratios obtained from the data, the extracted values of the baryonic entropy S/A for $\rho = 0.3\rho_0$, and the isotropic collective-flow energy E^F used in the calculations, as well as the corresponding values of the temperature T, are shown in Tables I and II.

Figures 6 and 7 show the quality of the data reproduction. The measured charge distributions dM/dZ and the distributions obtained using the FREESCO at an incident energy of 150A MeV are shown in Fig. 6. The measured kinetic-energy spectra for the angular range between 25° and 45° in the center-of-mass system and the spectra calculated using the FREESCO are shown in Fig. 7. For comparison, we also show the expected spectra from a purely thermal source. This thermal model does not reproduce the high kinetic energies of the heavier fragments.

The extracted entropy values will be discussed in the next section.

IV. DISCUSSION

The results reported in Tables I and II show that over the energy range (100–400)A MeV, the S/A values obtained using $(\sum_2^{15} M_i Z_i)/M_H$ vary from 1.4 to 2.6 for $(y \geq 0)_{\text{c.m.}}$ and from 1.1 to 2.2 for $(0 \leq y \leq 0.6y_p)_{\text{c.m.}}$. Using the evaluated neutron-to-proton ratio n/p, the obtained S/A values vary from 1.6 to 3.0 for the whole half-space of rapidity $(y \geq 0)_{\text{c.m.}}$ and from 1.2 to 2.6 for the midrapidity region $(0 \leq y \leq 0.6y_p)_{\text{c.m.}}$. These results are shown in Fig. 8, together with the results of Doss *et al.* [9] and the results of the earlier analysis of the FOPI Collaboration data performed by Kuhn *et al.* [12]. The results of calculations corresponding to, respectively, a fireball source [29] and two hydrodynamic models [13, 30] are also shown in the figure.

The following conclusions may be drawn.

(i) It appears that the S/A values extracted from the analysis of lighter species ($Z \leq 2$) [9] are higher than those obtained when IMF's are included in the analysis [12]; this behavior was observed earlier [31, 32]. In Fig. 8, the diamonds represent the experimental S/A values [9] obtained from the d-, t-, ^{3}He-, and ^{4}He-to-proton yield ratios for a finite reduced multiplicity $N_p/N_p^{\max}$, where N_p is the participant-proton multiplicity defined as

$$N_p = p + d + t + 2(^3\text{He} + ^4\text{He}), \tag{7}$$

and $N_p^{\max}$ is the maximum protonlike multiplicity taken at the lower limit of PM5 [33]. High values of entropy extracted from the analysis of lighter species were also reported in [6, 8, 10]. On the other hand, our n/p ratios obtained from the data via Eq. (6) depend not only on $(\sum_2^{15} M_i Z_i)/M_H$ (all particles and fragments with $Z \leq 15$), but also explicitly on the d/p and t/p ratios ($Z = 1$) calculated using the telescope data. Thus it is understandable that the S/A values extracted from the n/p ratios lie somewhere in between those obtained using light species only and those obtained using the IMF.

(ii) The entropies extracted from the $(\sum_2^{15} M_i Z_i)/M_H$ ratios are systematically lower than those extracted from the deduced n/p ratios. In the region of overlap they

TABLE I. Baryonic entropy S/A determined from central Au + Au collisions at beam energies of (100–400)A MeV from comparison of the measured ratio of the total charge bound in fragments with Z between 2 and 15 to hydrogen, $(\sum_2^{15} M_i Z_i)/M_H$, with the same ratio calculated using the modified FREESCO for a freeze-out density $\rho = 0.3\rho_0$, for the two rapidity conditions used. The values of the isotropic collective-flow energy E^F used in the calculation and the corresponding values of the temperature T are also reported.

E (A MeV)	y	$\left(\sum_2^{15} M_i Z_i\right)/M_H$	E^F (A MeV)	T (MeV)	S/A
100	$(y \geq 0)_{\text{c.m.}}$	2.65	9.59	5.4	1.4
	$(0 \leq y \leq 0.6y_p)_{\text{c.m.}}$	4.28 ± 0.80	11.0 ± 0.43	3.8 ± 0.4	1.1 ± 0.1
150	$(y \geq 0)_{\text{c.m.}}$	1.87	19.6	7.7	1.8
	$(0 \leq y \leq 0.6y_p)_{\text{c.m.}}$	2.72	21.6	5.4	1.5
250	$(y \geq 0)_{\text{c.m.}}$	1.15	38.7	12.2	2.2
	$(0 \leq y \leq 0.6y_p)_{\text{c.m.}}$	1.56	42.3	8.4	1.9
400	$(y \geq 0)_{\text{c.m.}}$	0.74	66.9	17.0	2.6
	$(0 \leq y \leq 0.6y_p)_{\text{c.m.}}$	0.98	73.8	11.7	2.2

generally agree with the entropies reported in Ref. [12], which were extracted from the same set of experiments using also charges up to $Z \sim 15$, but with the QSM as a theoretical background. Although not surprising, since the basic equivalence of the FREESCO and the QSM was pointed out earlier [15], this result is gratifying in view of the additional filtering allowed by the FREESCO. The charge distributions dM/dZ from the QSM are close to the distributions obtained from the FREESCO without filter (Fig. 1); hence they support the data extrapolation performed in Ref. [12].

(iii) For both variables [the measured $(\sum_2^{15} M_i Z_i)/M_H$ ratio and the deduced n/p ratio] and at all energies, the S/A values obtained from the midrapidity region $(0 \leq y \leq 0.6y_p)_{\text{c.m.}}$ are systematically lower by about 20% than the values obtained from $(y \geq 0)_{\text{c.m.}}$. ERAT5

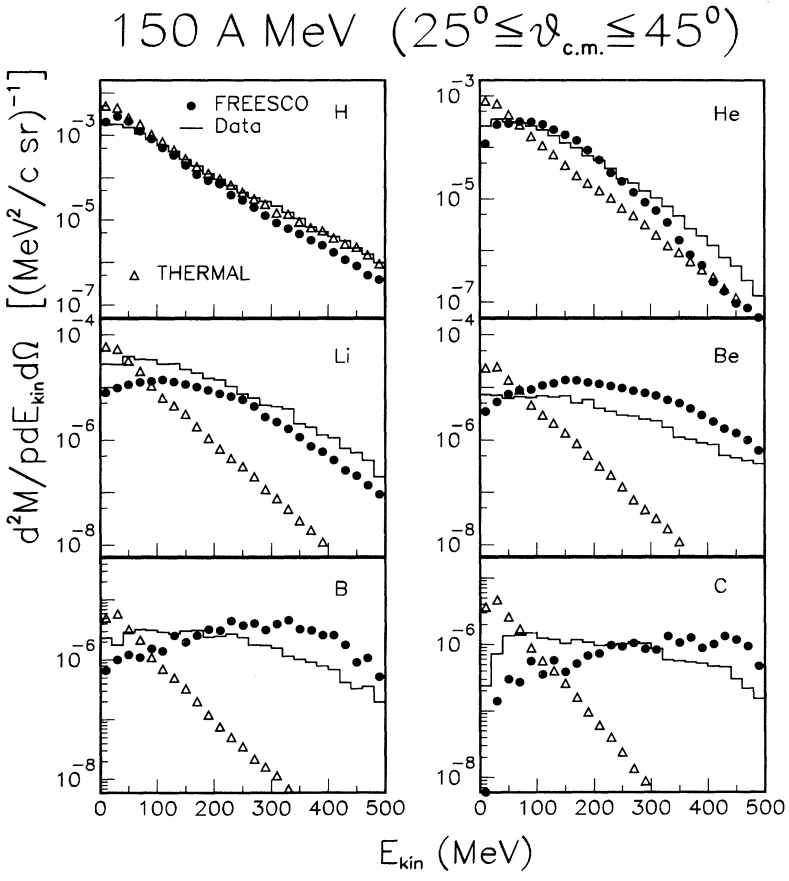

FIG. 7. Kinetic-energy distributions in the center-of-mass system, $d^2M/pdEd\Omega$, for different charges Z = 1–6 at an incident energy of 150A MeV. The measured spectra are shown as histograms and the spectra from the FREESCO as full circles. For comparison, the spectra from a thermal source are shown as triangles.

TABLE II. Same as Table I for the neutron-to-proton ratio n/p evaluated from the data via Eq. (6).

E (A MeV)	y	n/p	E^F (A MeV)	T (MeV)	S/A
100	$(y \geq 0)_{\text{c.m.}}$	5.34	8.64	6.4	1.6
	$(0 \leq y \leq 0.6y_p)_{\text{c.m.}}$	9.50 ± 1.40	10.8 ± 0.5	4.0 ± 0.5	1.2 ± 0.1
150	$(y \geq 0)_{\text{c.m.}}$	3.97	16.7	10.4	2.1
	$(0 \leq y \leq 0.6y_p)_{\text{c.m.}}$	5.89	20.1	7.0	1.7
250	$(y \geq 0)_{\text{c.m.}}$	2.79	32.7	16.8	2.6
	$(0 \leq y \leq 0.6y_p)_{\text{c.m.}}$	3.64	39.0	11.8	2.2
400	$(y \geq 0)_{\text{c.m.}}$	2.22	60.6	22.0	3.0
	$(0 \leq y \leq 0.6y_p)_{\text{c.m.}}$	2.43	67.5	16.8	2.6

also selects a small fraction of peripheral and semicentral collisions; hence, we expect that the difference of baryonic entropies for the two rapidity regions would be even higher for collisons with an impact parameter $b = 0$ fm than for collisions actually selected by ERAT5. Figure 9 shows that the values of $(\sum_2^{15} M_i Z_i)/M_H$ for the midrapidity region increase with ERAT (i.e., decrease with the impact parameter). Thus, for central collisons ($b = 0$ fm), the variable $(\sum_2^{15} M_i Z_i)/M_H$ in the midrapidity region is expected to be higher than the value obtained using ERAT5. In contrast, for $(y \geq 0)_{\text{c.m.}}$, the $(\sum_2^{15} M_i Z_i)/M_H$ ratio is almost constant with ERAT. Now, from Fig. 4 we conclude that S/A for the midrapidity region for ideally central collisions can only be lower than that obtained using ERAT5, i.e., the difference of baryonic entropies in the two rapidity regions is at least 20%. This difference cannot be accounted for by the experimental uncertainty of the data, since a 20% difference in S/A would require an average variation of $\approx 45\%$ in the variable $(\sum_2^{15} M_i Z_i)/M_H$, which is far outside the experimental error.

The 20% difference, however, could stem from the simplicity of the model used (FREESCO), which assumes the same, distance independent flow and temperature for all

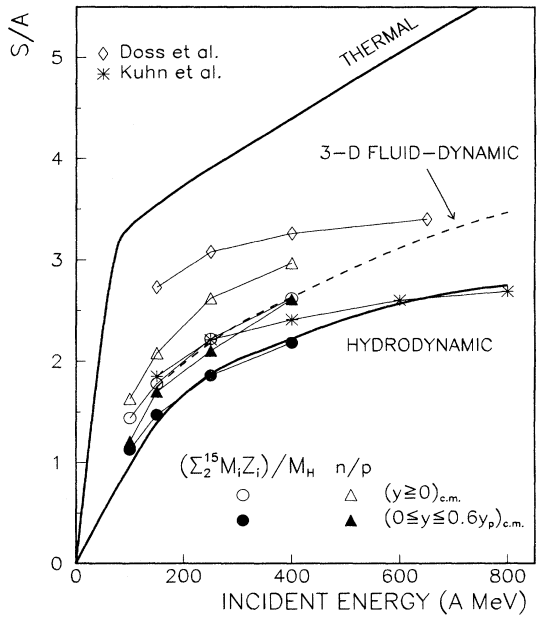

FIG. 8. Baryonic entropies S/A plotted as a function of beam energy. The earlier results of Doss *et al.* [9] are shown as diamonds and those of Kuhn *et al.* [12] as asterisks. The present results obtained from comparison with the FREESCO calculations are shown as circles and triangles. The circles represent S/A obtained from the $(\sum_2^{15} M_i Z_i)/M_H$ ratio and the triangles correspond to S/A obtained from the evaluated n/p ratio. The open symbols correspond to $(y \geq 0)_{\text{c.m.}}$ and the full symbols to $(0 \leq y \leq 0.6y_p)_{\text{c.m.}}$. The solid curve labeled THERMAL is calculated from the fireball model [29], the other solid curve, labeled HYDRODYNAMIC, from a very hard equation of state [30], and the dashed curve from a 3D fluid-dynamic calculation [13]. The thin solid curves connecting the extracted values of S/A are to guide the eye.

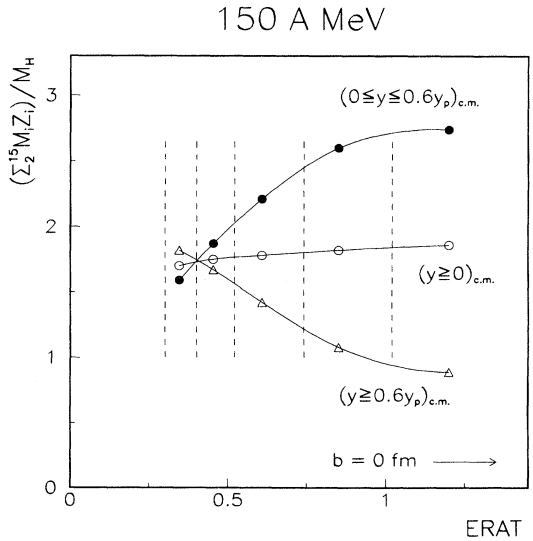

FIG. 9. Ratio of the total charge bound in fragments with Z between 2 and 15 to hydrogen production, $(\sum_2^{15} M_i Z_i)/M_H$, for different ERAT bins at an incident energy of 150A MeV for three rapidity conditions: (i) $(0 \leq y \leq 0.6y_p)_{\text{c.m.}}$ (full circles), (ii) $(y \geq 0)_{\text{c.m.}}$ (open circles), and (iii) $(y \geq 0.6y_p)_{\text{c.m.}}$ (triangles). The dashed lines represent the different ERAT bins used.

the emitted fragments. Further work on nonequilibrium in central heavy-ion collisions appears to be necessary.

Figure 8 shows that the extracted values of entropy agree well with hydrodynamic predictions [13, 30]. The solid curve in Fig. 8 corresponds to a hard equation of state (K=550 MeV) and the dashed one to a three-dimensional (3D) fluid-dynamic calculation [13]. The discrepancy between the entropies obtained in this paper and those calculated from the fireball model [29] (which assumes that all of the initial center-of-mass energy is converted into thermal energy) points out the importance of including the collective-motion component for a better understanding of the mechanism of relativistic heavy-ion collisions. As seen from Tables I and II, the collective-flow energies represent about 60% of the available energy per nucleon in the center of mass. For instance, this fraction is $\approx$ 65% at 150A MeV. In the calculation equal flow for all particles is assumed; however, as seen in Fig. 7, heavier particles would require a lower flow, whereas lighter particles would require the same or slightly higher flow than that reported in this paper. This finding supports the results obtained by Jeong *et al.* [27].

Assuming a freeze-out density, the extracted values of the baryonic entropy yield model values of the temperature. Figure 10 and Tables I and II show the results of the modified FREESCO calculations. For the chosen density $\rho = 0.3\rho_0$, the obtained temperatures increase from 3.8 to 11.7 MeV for $(0 \leq y \leq 0.6y_p)_{\text{c.m.}}$ and from 5.4 to 17 MeV for $(y \geq 0)_{\text{c.m.}}$, over the energy range (100–400)A MeV. As expected, Kuhn *et al.* report comparable values of the associated temperatures. Similar values have been reported by Wada *et al.* [10].

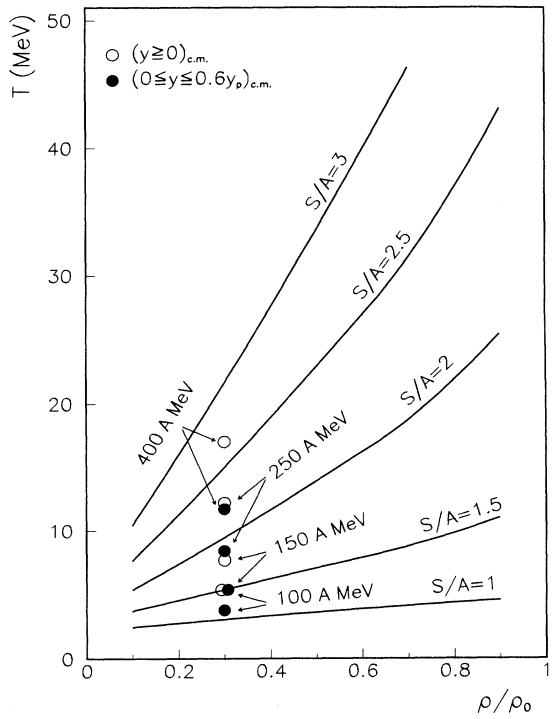

FIG. 10. Isentropic curves (constant S/A) calculated with the modified FREESCO, for S/A= 1 to 3 in steps of 0.5. Temperatures at the freeze-out density $\rho = 0.3\rho_0$, determined from comparison of the experimental observable $(\sum_2^{15} M_i Z_i)/M_H$ with the same quantity calculated using the modified FREESCO, are shown as open circles for $(y \geq 0)_{\text{c.m.}}$ and full circles for $(0 \leq y \leq 0.6y_p)_{\text{c.m.}}$.

V. SUMMARY AND CONCLUSIONS

In this study of Au + Au reactions at projectile energies of 100A, 150A, 250A, and 400A MeV we have extracted baryonic entropies for two rapidity regions. We have used two variables for this purpose: the experimental value of the yield ratio of the total charge bound in fragments with Z between 2 and 15 to hydrogen production, $(\sum_2^{15} M_i Z_i)/M_H$, and the neutron-to-proton yield ratio n/p evaluated from the FOPI data via Eq. (6). These ratios have then been compared with the corresponding ones calculated using the modified FREESCO [23,34,35], assuming a freeze-out density $\rho = 0.3\rho_0$.

The following conclusions may be drawn.

(i) The analysis has allowed for the simultaneous extraction of the baryonic entropy, temperature, and flow.

(ii) The entropy values extracted in this work are in overall agreement with those obtained in the recent paper by Kuhn *et al.* [12] who used the QSM, and are in fair agreement with a recent hydrodynamic calculation by Schmidt *et al.* [13].

(iii) The high values of the collective-flow energy obtained in the analysis confirm the importance of collective motion in relativistic heavy-ion collisions and are in agreement with the values obtained by Jeong *et al.* [27] and Reisdorf [36].

(iv) Entropies extracted from the midrapidity region for purely central collisions, at all incident energies, are found to be systematically lower by at least $\approx$ 20% than those extracted from the full rapidity hemisphere.

ACKNOWLEDGMENTS

It is a pleasure to thank J. Konopka for interesting discussions and stimulating suggestions. One of us (M.Dž.) expresses his gratitude to Dr. K.D. Hildenbrand and all the members of the FOPI Collaboration for the kind hospitality extended during his stay at the GSI, Darmstadt. He also thanks the Deutscher Akademischer Austauschdienst for financial support of his stay at GSI, Darmstadt. Finally, the Zagreb group gratefully acknowledges the financial support of the Internationales Büro der KfA Jülich.

APPENDIX

Let $\sum_{\text{all } Z} M_i A_i$ be the total number of nucleons within a given phase space encompassed in nuclei with $Z \geq 1$ (i.e., the emitted neutrons are not counted in the sum), where A_i and M_i are, respectively, the mass number and the multiplicity of a species i. Supposing that, for all emitted charged fragments with $2 \leq Z \leq 15$,

$A = 2Z$, we have

$$\sum_{\text{all } Z} M_i A_i = \sum_{Z=1} M_i A_i + 2 \sum_{Z=2}^{15} M_i Z_i + \sum_{Z \geq 15} M_i A_i. \tag{A1}$$

The first term on the right-hand side can be calculated as

$$\sum_{Z=1} M_i A_i = \langle A_H \rangle M_H = \frac{p + 2d + 3t}{p + d + t} M_H = \frac{1 + 2d/p + 3t/p}{1 + d/p + t/p} M_H, \tag{A2}$$

where p, d, t, and $M_H = p + d + t$ are, respectively, the proton, deuteron, triton, and hydrogen-isotope multiplicities.

For the particular case of a Au + Au collision, we assume that, for the same part of the phase space, the following relation is valid:

$$\frac{n + \sum_{\text{all } Z} M_i A_i}{\sum_{\text{all } Z} M_i Z_i} = \frac{A_{\text{Au}}}{Z_{\text{Au}}}. \tag{A3}$$

Here, n is the number of emitted free neutrons, and $A_{\text{Au}} = 197$ and $Z_{\text{Au}} = 79$ are, respectively, the mass and the atomic numbers of gold.

From Eq. (A3), the number of free neutrons n is

$$n = \frac{A_{\text{Au}}}{Z_{\text{Au}}} \sum_{\text{all } Z} M_i Z_i - \sum_{\text{all } Z} M_i A_i, \tag{A4}$$

and dividing it by the number of emitted free protons p

$$p = \frac{M_H}{(1 + d/p + t/p)}, \tag{A5}$$

and using Eqs. (A1) and (A2), one easily obtains the n/p ratio as

$$n/p = \frac{A_{\text{Au}}}{Z_{\text{Au}}} \left(1 + \frac{d}{p} + \frac{t}{p}\right) \left(1 + \frac{\sum_2^{15} M_i Z_i}{M_H}\right) - \left(1 + 2\frac{d}{p} + 3\frac{t}{p}\right) - 2\left(1 + \frac{d}{p} + \frac{t}{p}\right) \frac{\sum_2^{15} M_i Z_i}{M_H} + \left(1 + \frac{d}{p} + \frac{t}{p}\right) \frac{\sum_{Z \geq 15} M_i \left(\frac{A_{\text{Au}}}{Z_{\text{Au}}} - A_i\right)}{M_H}. \tag{A6}$$

Since the multiplicity fragment distribution, dM/dZ, falls exponentially with Z, the last term is much smaller than the rest of the n/p ratio. Thus we can neglect it and for the evaluated n/p ratio we have

$$n/p \approx \frac{197}{79} \left(1 + \frac{d}{p} + \frac{t}{p}\right) \left(1 + \frac{\sum_2^{15} M_i Z_i}{M_H}\right) - \left(1 + 2\frac{d}{p} + 3\frac{t}{p}\right) - 2\left(1 + \frac{d}{p} + \frac{t}{p}\right) \frac{\sum_2^{15} M_i Z_i}{M_H}. \tag{A7}$$

The value of $(\sum_2^{15} M_i Z_i)/M_H$ is obtained using the data from the outer plastic wall and its ionization-chamber cluster detector. The d/p and t/p ratios are determined using the telescopic data extrapolated to the same solid angle as subtracted by the charged-particle detectors (full azimuth and polar angle between 7° and 30° lab).

[1] I.M. Mishustin, F. Myhrer, and P.J. Siemens, Phys. Lett. **95B**, 361 (1980).

[2] P.J. Siemens and J.I. Kapusta, Phys. Rev. Lett. **43**, 1486 (1979).

[3] G.F. Bertsch, Nucl. Phys. **A400**, 221c (1983).

[4] S. Nagamiya, M.C. Lemaire, E. Möller, S. Schnetzer, G. Shapiro, H. Steiner, and I. Tanihata, Phys. Rev. C **24**, 971 (1981).

[5] B.V. Jacak, G.D. Westfall, C.K. Gelbke, L.H. Harwood, W.G. Lynch, D.K. Scott, H. Stöcker, M.B. Tsang, and T.J.M. Symons, Phys. Rev. Lett. **51**, 1846 (1983).

[6] H.H. Gutbrod, H. Löhner, A.M. Poskanzer, T. Renner, H. Riedesel, H.G. Ritter, A. Warwick, F. Weik, and H. Wieman, Phys. Lett. **127B**, 317 (1983).

[7] B.V. Jacak, H. Stöcker, and G.D. Westfall, Phys. Rev. C **29**, 1744 (1984).

[8] K.G.R. Doss, H.A. Gustafsson, H.H. Gutbrod, B. Kolb, H. Löhner, B. Ludewigt, A.M. Poskanzer, T. Renner, H. Riedesel, H.G. Ritter, A. Warwick, and H. Wieman, Phys. Rev. C **32**, 116 (1985).

[9] K.G.R. Doss, H.A. Gustafsson, H.H. Gutbrod, D. Hahn, K.H. Kampert, B. Kolb, H. Löhner, A.M. Poskanzer, H.G. Ritter, H.R. Schmidt, and H. Stöcker, Phys. Rev. C **37**, 163 (1988).

[10] R. Wada, K.D. Hildenbrand, U. Lynen, W.F.J. Müller, H.J. Rabe, H. Sann, H. Stelzer, W. Trautmann, R. Trockel, N. Brummund, R. Glasow, K.H. Kampert, R. Santo, E. Eckert, J. Pochodzalla, I. Bock, and D. Pelte,

Phys. Rev. Lett. **58**, 1829 (1987).
[11] D. Hahn and H. Stöcker, Nucl. Phys. **A476**, 718 (1988).
[12] C. Kuhn, FOPI Collaboration at GSI, and J. Konopka, Phys. Rev. C **48**, 1232 (1993).
[13] W. Schmidt, B. Waldhauser, H. Stöcker, J.A. Maruhn, and W. Greiner, Phys. Rev. C **47**, 2782 (1993).
[14] G. Fai and J. Randrup, Comput. Phys. Commun. **42**, 385 (1986).
[15] L.P. Csernai, J.I. Kapusta, G. Fai, D. Hahn, J. Randrup, and H. Stöcker, Phys. Rev. C **35**, 1297 (1987).
[16] A. Gobbi and the FOPI Collaboration at GSI, Nucl. Instrum. Methods Phys. Res. Sect. A **324**, 156 (1993).
[17] G. Poggi, G. Pasquali, M. Bini, P.R. Maurenzig, A. Olmi, and N. Taccetti, Nucl. Instrum. Methods Phys. Res. Sect. A **324**, 177 (1993).
[18] J.P. Coffin for the FOPI Collaboration at GSI, Int. J. Mod. Phys. E **1**, 739 (1992).
[19] J.P. Alard and the FOPI Collaboration at GSI, Phys. Rev. Lett. **69**, 889 (1992).
[20] P. Beckmann, H.A. Gustafsson, H.H. Gutbrod, K.H. Kampert, B. Kolb, H. Loehner, A.M. Poskanzer, H.G. Ritter, H.R. Schmidt, and T. Siemiarczuk, Mod. Phys. Lett. A **2**, 163 (1987).
[21] R. Bock, G. Claesson, K.G.R. Doss, R.L. Ferguson, I. Gavron, H.A. Gustafsson, H.H. Gutbrod, J.W. Harris, B.V. Jacak, K.H. Kampert, B. Kolb, P. Kristiansson, F. Lefebvres, A.M. Poskanzer, H.G. Ritter, H.R. Schmidt, T. Siemiarczuk, L. Teitelbaum, M. Tincknell, S. Weiss, H. Wieman, and J. Wilhelmy, Mod. Phys. Lett. A **2**, 721 (1987).
[22] W. Reisdorf for the FOPI Collaboration at GSI, in *Proceedings of the XX International Workshop on Gross Properties of Nuclei and Nuclear Excitation*, Hirschegg, Austria, 1992, edited by H. Feldmeier (GSI and Institut für Kernphysik, Technische Hochschule, Darmstadt, 1992), p. 38.
[23] J. Randrup and S.E. Koonin, Nucl. Phys. **A356**, 223 (1981).
[24] Z.G. Fan, A. Gobbi, N. Herrmann, and J. Randrup, GSI Scientific Report No. 1992–1, 1992.
[25] C.M. Lederer and V.S. Shirley, *Table of Isotopes* (Wiley, New York, 1978).
[26] J. Randrup, Comp. Phys. Commun. **77**, 153 (1993).
[27] S.C. Jeong, the FOPI Collaboration at GSI, and J. Randrup, Phys. Rev. Lett. **72**, 3468 (1994).
[28] S. Hölbling, "Detector Acceptance Filter," FOPI Collaboration reference library report, 1992.
[29] J. Gosset, H.H. Gutbrod, W.G. Mayer, A.M. Poskanzer, A. Sandoval, R. Stock, and G.D. Westfall, Phys. Rev. C **16**, 629 (1977).
[30] H. Stöcker, M. Gyulassy, and J. Boguta, Phys. Lett. **103B**, 269 (1981).
[31] L.P. Csernai, G. Fai, and G.D. Westfall, Phys. Rev. C **38**, 2681 (1988).
[32] R. Trockel, K.D. Hildenbrand, U. Lynen, W.F.J. Müller, H.J. Rabe, H. Sann, H. Stelzer, W. Trautmann, E. Eckert, J. Pochodzalla, and N. Brummund, Phys. Rev. C **38**, 576 (1988).
[33] K.G.R. Doss, H.A. Gustafsson, H.H. Gutbrod, K.H. Kampert, B. Kolb, H. Löhner, B. Ludewigt, A.M. Poskanzer, H.G. Ritter, H.R. Schmidt, and H. Wieman, Phys. Rev. Lett. **57**, 302 (1986).
[34] G. Fai and J. Randrup, Nucl. Phys. **A381**, 557 (1982).
[35] G. Fai and J. Randrup, Nucl. Phys. **A404**, 551 (1983).
[36] W. Reisdorf for the FOPI Collaboration at GSI, in *Proceedings of the XXII International Workshop on Gross Properties of Nuclei and Nuclear Excitation*, Hirschegg, Austria, 1994, edited by H. Feldmeier and W. Nörenberg (GSI, Darmstadt, 1994), p. 93.